Desalination and Water Treatment
www.deswater.com

doi: 10.5004/dwt.2017.1482

60 (2017) 242–248
January

Photocatalytic degradation of methyl orange by chitosan/CdS nanoparticle composite films

Tao Feng[a,b,*], Tingting Zhao[a], Lei Xu[a], Baolin Deng[b]

[a]*College of Resources and Environmental Engineering, Wuhan University of Science and Technology, Wuhan 430081, China, Tel./Fax: +86 27 68862877; emails: fengtaowhu@163.com (T. Feng), ttzhaowust@163.com (T. Zhao); xuleiwust@163.com (L. Xu)*
[b]*Department of Civil and Environmental Engineering, University of Missouri, Columbia, MO, 65211 USA, Tel. +1 573 8820075; Fax: +1 573 8824784; email: dengb@missouri.edu (B. Deng)*

Received 30 September 2015; Accepted 6 July 2016

ABSTRACT

Cadmium sulfide (CdS) nanoparticles were synthesized *in situ* in the presence of chitosan hydrogel films. The resulting chitosan/CdS nanoparticle composite films were characterized by Fourier transform infrared spectroscopy (FTIR) and transmission electron microscopy (TEM). The photocatalytic reactivity of the chitosan/CdS nanoparticle composite films was evaluated using methyl orange (MO) as a model pollutant. The influence of various parameters towards MO degradation was investigated including the amount of the catalyst, initial MO concentration, pH and the catalytic cycles. The decolorization efficiency was 90% in this study, and after four times reuse, the efficiency still remained high at 78.2%. The study demonstrated that the crosslinked chitosan hydrogel films provided a confined matrix for the growth of CdS nanoparticles and the coordination of Cd^{2+} with $–NH_2$ groups in C_2 and –OH groups in C_3 of the chitosan chain likely occurred. The photocatalytic decolorization of MO was found to follow a pseudo-first-order kinetics according to the Langmuir–Hinshelwood (L-H) model. The UV-vis spectroscopy study indicated that the aromatic rings (with a peak at 270.0 nm) and azo bonds (with a peak at 463.0 nm) of MO were broken under the UV light irradiation in the presence of the chitosan/CdS nanoparticle composite film.

Keywords: Cadmium sulfide; Chitosan; Photocatalytic degradation; Methyl orange

1. Introduction

Different techniques have been developed to remove organic pollutants in wastewater, such as flocculation precipitation, absorption and photocatalytic degradation [1–4]. Photocatalysis is one of the major approaches used for the degradation of organic pollutants in wastewater [5,6]. Reports of complete decomposition of organic pollutants through photocatalysis using metal oxide semiconductors are abundant under UV light irradiation [7,8]. Photo excitation of semiconductors generates electron-hole pairs capable of attacking organic dyes either directly by the strongly oxidative holes or indirectly by other reactive species generated by their reactions with the solvent and/or additives [9].

Cadmium sulfide (CdS), with a direct band gap of 2.4 eV, has long been recognized as an important semiconductor for contaminant degradation [10]. The unique photochemical and photophysical properties of the CdS nanoparticles had been exploited for efficient photocatalytic degradation of organic pollutants [11]. Prasad et al. [12] prepared CdS nanoparticles under various ultrasonic operating conditions and evaluated their photocatalytic reactivity towards Reactive Blue 4. Challenges involved in such applications are the potential leaching of CdS particles that may result

* Corresponding author.

Contract Grant Sponsor: National Natural Science Foundational of China (50904047); Hubei Provincial Department of Education (D20141106).

in secondary Cd^{2+} pollution and poor recyclability of CdS as a photocatalyst [13]. To overcome these problems, immobilizing CdS nanoparticle into supporting materials has been adopted. Huo et al. [14] synthesized CdS-TiO_2 photocatalyst via *in situ* sulfurization of doped TiO_2 under supercritical conditions. The strong interaction between CdS and TiO_2 could efficiently protect the CdS from photocorrosion and leaching. Xiao et al. [15] synthesized CdS quantum dots/grapheme nanosheets hybrid films and explored the photocatalytic degradation of aromatic nitro compounds. Recently, synthesis of CdS nanoparticles in polymer matrices has been explored, which has the advantage of effectively suppressing the photocorrosion of CdS during photochemical reaction [16]. The ability of polymer matrices to suppress the photoleaching of CdS is important because we need to prevent the release of toxic Cd^{2+} into the treated water.

Chitosan is the N-deacetylation product of chitin, the second most abundant naturally-occurring biopolymer next to cellulose. The material could be a very suitable matrix to prepare CdS nanoparticle composite because (1) chitosan is non-toxic and biodegradable so its application is considered green; (2) it has a strong chelating ability with transition metal ions such as Cd^{2+}, which is desirable as a template of nanoparticle synthesis; (3) the amino and hydroxyl groups on linear chitosan chains are good capping groups for CdS nanoparticles and at the same time, the highly viscous nature of chitosan might prevent CdS nanoparticles from agglomeration, uncontrolled growth, and photoleaching; and (4) chitosan possesses a unique three-dimensional structure of molecules with a high chemical reactivity and favorable particle- and film-forming property. Reports exist to use chitosan as a host to biosynthesize nanosized TiO_2, ZnS, CdS, etc. [17].

In this study, chitosan/CdS nanoparticle composite films were prepared by synthesizing CdS nanoparticles in the natural polysaccharide template. The resulting composite films were characterized by Fourier transform infrared spectroscopy (FTIR) and transmission electron microscopy (TEM). The photocatalytic decolorization of MO in the aqueous solution was carried out to evaluate the photocatalytic activities of chitosan/CdS nanoparticles composite films under UV-light irradiations.

2. Materials and methods

2.1. Materials

Chitosan was purchased from Zhejiang Ocean Biochemical. The degree of deacetylation was 90% and the molecular weight calculated from gel permeation chromatograph (GPC) was 2.3×10^5. Methyl orange (MO), cadmium chloride and sodium sulfide were of analytical grade. All solutions were prepared by distilled water.

2.2. Preparation of Chitosan/CdS Nanoparticle Composite Film

Firstly, 2 g of chitosan was dissolved into 100 mL acetic acid solution (2%, v/v) with vigorous stirring. Then, 0.668 g of $CdCl_2$ was dissolved into 20 mL distilled water with mild stirring. Subsequently, $CdCl_2$ solution was mixed with 50 mL chitosan acetic acid solution followed by continuous stirring for 10 h to allow chelation of chitosan molecules with Cd^{2+}. The resulting solution was filtered, degassed, and then spread over a glass plate for film formation. After drying at room temperature, the glass plates with the film were immersed into Na_2S solution, leading to the formation of CdS nanoparticles within the chitosan film matrix. The wet films desquamated from glass plates were washed with a saturated NaCl solution and dried under vacuum prior to characterization and testing [18]. The amount of Cd^{2+} loaded in chitosan film was 0.08 g g^{-1}, determined by a GGX-9 atomic absorption spectrometer (Haiguang, China).

2.3. Characterization

FTIR spectra of the powdered samples were recorded on Nicolet-360 FT-IR spectrometer with KBr pellet. The TEM micrographs were obtained by a JEOL JEM-2100 transmission electron microscope machine (Tokyo, Japan) at an accelerating voltage of 200 kV. The UV–vis absorption spectra of treated MO solutions were recorded using a Shimadzu UV-2550 UV–visible spectrophotometer. The X-ray diffraction (XRD) patterns of the films were measured by a D/max-rA (Tokyo, Japan) diffractometer with Cu target and Ka radiation at 40 kV and 50 mA.

2.4. Photocatalytic reaction

The photocatalytic activities of chitosan/CdS nanoparticle composite films were evaluated based on the photodegradation of aqueous MO with or without the composite film. A certain amount of the catalyst was dispersed into 100 ml of MO solution in a plastic flask, which was then placed at 10 cm below an UV lamp (a 50 W Hg lamp) for irradiation under different time durations (from 0 to 240 min). The MO concentration in the aqueous solution was monitored by measuring the absorbance at 463 nm. The decolorization efficiency was then calculated according to Eq. (1):

$$\text{Decolorization efficiency (\%)} = \frac{C_0 - C}{C_0} \times 100\% \quad (1)$$

where C is the MO concentration at reaction time t (min), and C_0 is the initial MO concentration (mg L^{-1}).

It has been reported that the photocatalytic decolorization rates of various dyes follow the Langmuir–Hinshelwood (L–H) kinetics model below (Eq. (2)) [19]:

$$r = -\frac{dC}{dt} = \frac{kKC}{1+KC} \quad (2)$$

where k is the reaction rate constant (mg·L^{-1} min^{-1}); K is the adsorption coefficient of the reactant (L·mg^{-1}); and C is the reactant concentration (mg·L^{-1}). When the concentration C is very small, KC is negligible with respect to unity, and the photocatalysis can be simplified to an apparent pseudo-first-order kinetics (Eqs. (3) and (4)) [20]:

$$-\frac{dC}{dt} = kKC \quad (3)$$

$$\ln\left(\frac{C_0}{C}\right) = kKt = k_{app}.t \quad (4)$$

where k_{app} is the apparent pseudo-first-order rate constant (min^{-1}).

3. Results and discussion

3.1. Characterization of chitosan/CdS nanoparticle composite film

The FTIR spectra of pure chitosan and chitosan/CdS nanoparticles composite film are shown in Fig. 1(a). The absorption band at 1,600 cm^{-1} in chitosan is attributed to the N-H bending mode of $–NH_2$, and the peaks at 3,415 cm^{-1} are derived from the stretching vibrations of hydroxyl, amino and amide groups. Compared with pure chitosan, the wide peak at 3,415 cm^{-1} shifted to a lower frequency and became broader in the chitosan/CdS composite, indicating that $–NH_2$ or –OH groups took part in the reaction. Another interesting observation in FTIR spectra is that different functional groups of chitosan appear to interact differently with CdS. The peaks located at 1,074 cm^{-1} assigned to C_3-O stretching shifted to a lower wave number of 1,064 cm^{-1} due to the presence of CdS, while the peak at 1,600 cm^{-1} of N-H bending moved to a higher wave number 1,592 cm^{-1}. These changes suggested that $–NH_2$ group in C_2 and –OH group in C_3 were likely involved in the interaction with CdS. The chitosan hydrogel films provided a confined space in the polymer matrix for the growth of CdS nanoparticles, and coordination of Cd^{2+} with $–NH_2$ groups in C_2 and –OH groups in C_3 of the chitosan chain likely occurred.

The TEM image of a chitosan/CdS nanoparticle composite film (Fig. 1(b)) indicated that the obtained CdS nanoparticles were spherical and mostly monodispersed. The average diameter was 5.1 nm based on the calculation by the software ImageJ from a total of 48 particles. It was clear that the chitosan networks had effectively prevented the particles from further growth and aggregation.

The UV–visible absorption spectra of chitosan/CdS nanoparticles composite films are illustrated in Fig. 1(c). For bulk CdS, the absorption edges are located at 500 nm, corresponding to the energy band gaps of 2.5 eV. The absorption edge of CdS nanoparticle synthesized in chitosan film shows a clear blue shift, implying the quantum size confinement effect of the nanoscale particles [17].

XRD patterns of chitosan and chitosan/CdS nanoparticles composite film are shown in Fig. 1(d). The XRD pattern of chitosan consisted of two typical crystalline peaks at 2θ = 15.1° and 20.9°. For the chitosan/CdS nanoparticle composite film, there are three additional peaks corresponding to the (111), (220) and (311) planes of the cubic CdS phase [18]. Since CdS generally crystallizes in the thermodynamically

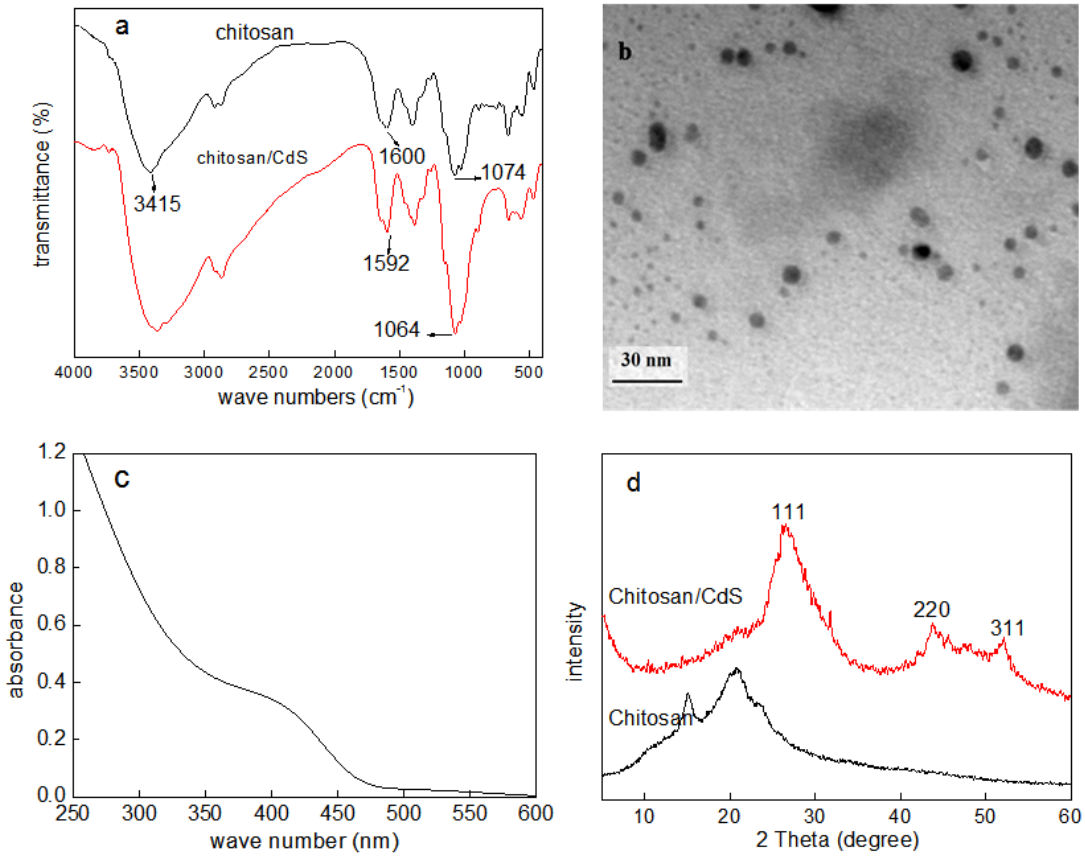

Fig. 1. (a) FTIR spectra of chitosan and chitosan/CdS nanoparticle composite film; (b) TEM image of the composite film; (c) Absorbance spectra of the composite film; (d) XRD patterns of chitosan and the composite film.

favored hexagonal structure in bulk form, one may infer that in the chitosan matrix CdS nanoparticles prefer the kinetically controlled cubic structure, and it is also proved that chitosan affects the CdS crystallizing process.

3.2. Decolorization and degradation of MO in different systems

Fig. 2 shows the decolorization of the MO solution in the system with only UV light irradiation, with chitosan/CdS nanoparticle composite film (0.7 g·L^{-1}) but in dark, and with chitosan/CdS nanoparticle composite film (0.7 g·L^{-1}) under visible light (a 300 W Xenon lamp (PLS-SEX300C) with a 400 nm cut-off filter.) or UV light irradiation, respectively. All testing systems contained 100 mL of MO solutions (15 mg·L^{-1}). The blank experiment under the UV light irradiation without catalyst measured only direct photolysis, which was found to be minimal during 120-min treatment. In the absence of UV light irradiation but with the chitosan/CdS nanoparticle composite film, the removal of MO could occur by sorption due to CdS nanoparticles and the residual –NH_2 and –OH groups in the chitosan. The result here showed a MO decolorization efficiency of 18.3% after 120 min of adsorption. When the MO solution was exposed to visible light in the presence of the chitosan/CdS nanoparticle composite film, about 24.8% of the dye was decolored within 120 min. However, after 120 min UV light irradiation about 74.7% of the dye was decolored. The decolorization efficiency showed a 56.4% increase when compared with the visible light system, so the UV light catalytic system was employed in this study. There should be simultaneously adsorption and photocatalytic degradation of MO on the nanocomposite film in the presence of UV light irradiation. The adsorption ability of chitosan/CdS nanoparticle composite film enhances the photocatalytic reactivity towards MO degradation, and synergistically, the photocatalysis and adsorption lead to dye decolorization [21].

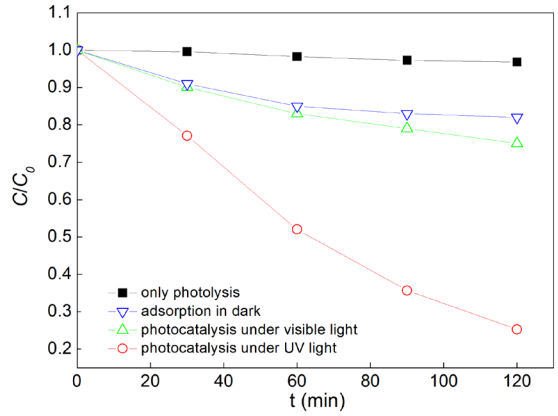

Fig. 2. Degradation of MO with time in different systems.

3.3. Photocatalytic process

To understand the molecular and structural changes of MO during its photocatalytic degradation, representative UV-vis spectra of the dye solution were collected as a function of reaction time [22,23]. As shown in Fig. 3(a), the primary adsorption peaks of the original dye solution were at 270.0 nm and 463.0 nm in the range of 200–560 nm. The peak at 270.0 nm was attributed to aromatic rings in the MO molecules and the visible peak at 463.0 nm was assigned to azo structure of the dye. During photocatalysis under the UV-light, the absorbance at 463.0 nm decreased from 1.03 to 0.33 with the time increase from 0 to 180 min. At the same time, the two absorption peaks at 270.0 nm and 463.0 nm shifted to 261.0 nm and 450.0 nm, respectively. The results indicate that the aromatic rings at 270.0 nm and azo bonds at 463.0 nm of MO were broken under UV light irradiation in the presence of 0.7 g·L^{-1} chitosan/CdS nanoparticle composite film. Similar phenomena have been observed during photocatalytic decolorization and degradation of Congo Red [24].

To confirm the degradation of MO, the total organic carbon (TOC) values of MO solution at different time under UV light irradiation and in dark in the presence of the catalyst was measured (Fig. 3(b)). The decrease of TOC at the beginning was due to the adsorption of MO onto the catalyst

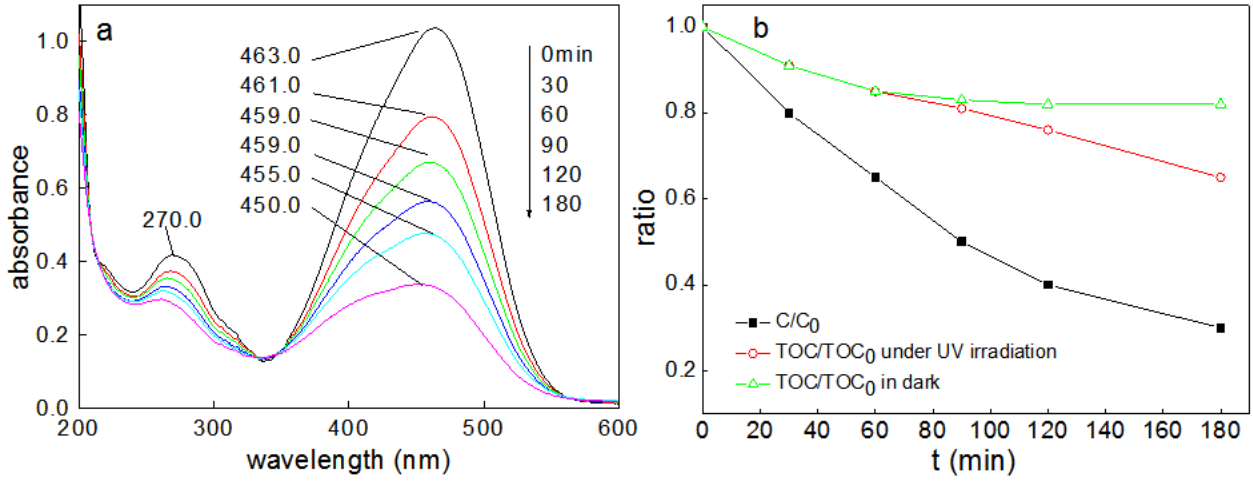

Fig. 3. Changes of methyl orange UV-vis spectra and TOC with reaction time.

surface. After 1 h, no obvious changes of TOC values were observed in dark with further prolong the time. However, the TOC values of MO solution decreased under the UV light irradiation. It means that, the molecule of MO was destructed during experiment. As shown in Fig. 3(b), MO concentration decreases more quickly than TOC value, suggesting that the intermediate products are more difficult to oxidize than their parent compound, and a complete oxidation proceeds at a much slower reaction rate [25].

During photocatalytic degradation process, the active species including superoxide radicals ($\bullet O_2^-$), holes (h+) and hydroxyl radicals (•OH) with powerful oxidation ability will be produced. To detect the active species during photocatalytic process, 10 mM isopropyl alcohol (IPA), methanol, and p-benzoquinone (BQ), which are known as effective •OH, holes, and $\bullet O_2^-$ scavengers, respectively, were added into MO solution in the control experiments [26,27]. As shown in Fig. 4, the decolorization efficiency of MO decreased slightly upon the addition of IPA and methanol, indicating that free hydroxyl radicals and the holes were not the main active species in this process. In contrast, the addition of BQ had a significantly negative effect on the decolorization of MO, confirming that the superoxide radicals were the dominant active species. Therefore, the main photocatalytic process can be proposed. Firstly, the photons with the energy higher than that of the CdS band gap are absorbed onto the CdS surface. This results in the excitation of the electrons from valence band (*vb*) to conduction band (*cb*), producing holes (h_{vb}^+) at the valence band edge and electrons (e_{cb}^-) in the conduction band (Eq. (5)). Subsequently, e_{cb}^- can react with the O_2 molecules to generate $\bullet O_2^-$ (Eq. (6)). Finally, the MO molecules are oxidized by $\bullet O_2^-$ and decomposed (Eq. (7)).

$$CdS + h\nu \rightarrow CdS(h_{vb}^+ + e_{cb}^-) \quad (5)$$

$$e_{cb}^- + O_2 \rightarrow H^+ + \bullet O_2^- \quad (6)$$

$$\bullet O_2^- + MO \rightarrow \text{degraded products} \quad (7)$$

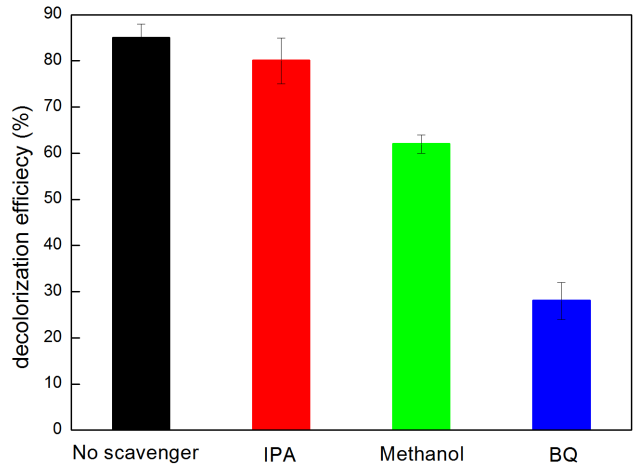

Fig. 4. Effects of various scavengers on decolorization of MO.

3.4. Effect of initial MO concentration on decolorization of MO

The effect of initial concentrations of MO on the photocatalytic degradation was investigated by varying the dye concentrations from 5 to 25 mg·L^{-1} (100 mL, pH 4.0) in the presence of 0.7 g·L^{-1} catalyst under the UV light irradiation for 3 h (Fig. 5). The decolorization efficiencies of dye were 86.8%, 79.3%, 78.7%, 70.9% and 53.7%, respectively, at the dye initial concentration of 5, 10, 15, 20 and 25 mg·L^{-1} after 180 min of irradiation. The percentage of decolorization decreased with increasing concentration of initial MO. At the same time, the system was stirred in dark for 180 min to measure the decolorization due to adsorption. The decolorization efficiencies of MO were 22.6%, 20.1%, 19.8%, 17.3% and 15.1% in the dark, respectively (data not shown).

Linear relationships between ln(C_0/C) and irradiation time were observed under different initial MO concentrations, indicating that reaction followed a pseudo-first-order kinetics (Fig. 5 (inset)). The rate constants (k_{app}) for the decolorization process were 1.10, 0.88, 0.86, 0.71 and 0.42 × 10^{-2} min^{-1} at 5, 10, 15, 20 and 35 mg·L^{-1} of initial MO concentrations, respectively. The photocatalytic degradation rate constant was observed to decrease with increasing initial MO concentration. It is likely that as the total dye concentration increases, the aqueous concentration of dye increases, leading to less penetration of light through the solution on to the surface of catalyst and less production of hydroxyl radical that is the primary reactive species for the dye degradation [28].

3.5. Effect of catalyst loading on decolorization of MO

The amount of photocatalyst in the system is another critical parameter determining the degradation efficiency. To investigate the effect of the chitosan/CdS nanocomposite film dosage on the photocatalytic degradation of MO, a series of experiments were conducted with varying catalyst amounts from 0.2 to 1 g·L^{-1} in 100 mL MO solution (initial concentration 15 mg·L^{-1}, pH 4.0) (Fig. 6). As the amount of photocatalyst was increased from 0.2 to 0.7 g·L^{-1}, the MO concentration in the solution decreased rapidly. The decolorization efficiency reached 90% after 240 min at a catalyst loading

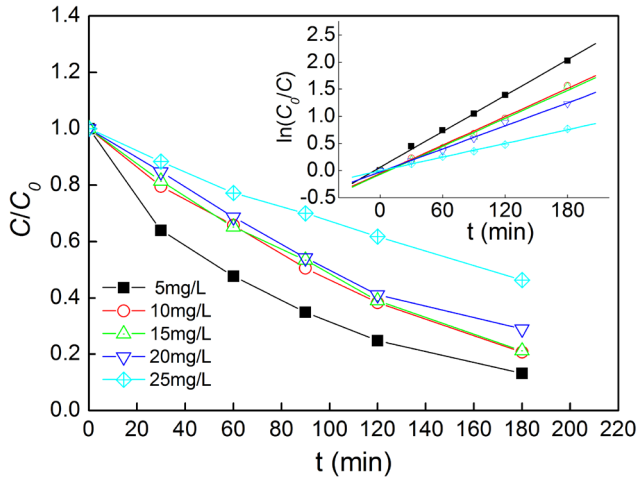

Fig. 5. Effect of MO concentration on decolorization of MO.

of 0.7 g·L^{-1}. At the same time, the decolorization due to the adsorption was measured. The decolorization efficiencies of MO were 8.6%, 15.1%, 20.3% and 23.4% in dark, respectively (data not shown). It is likely that with an increasing catalyst loading, the number of photons absorbed and the number of dye molecules adsorbed are increased. With a further increase of the loading beyond 0.7 g·L^{-1}, a negative effect on the decolorization efficiency of MO was observed. Light blocking by an excessive amount of catalyst may account for the decreased decolorization efficiency. With a lower degree of CdS illumination, less hydroxyl radicals were generated for the degradation of MO [29].

The apparent rate constants under different catalyst amounts could be obtained from the plots of In(C_0/C) versus irradiation time in Fig. 6 (inset). It can be clear that the highest photocatalytic efficiency occurred at 0.7 g·L^{-1} catalyst loading with a rate constant of 0.0096 min^{-1}.

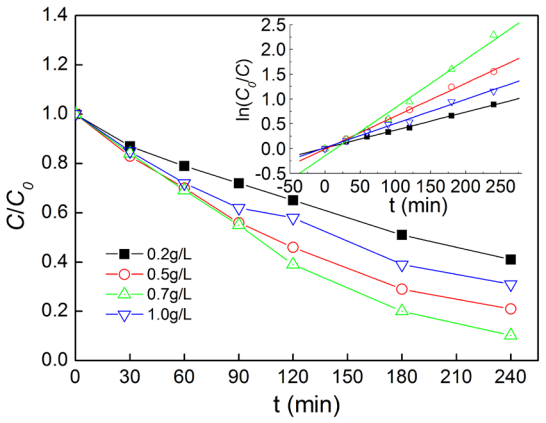

Fig. 6. Effect of catalyst loading on the decolorization of MO.

3.6. Effect of pH on the decolorization of MO

The solution pH generally plays an important role in the generation of hydroxyl radical, and thus the dye decolorization efficiency. The photocatalytic decolorization of MO solution (15 mg·L^{-1}) under different pH values of 3.0, 6.0 and 10.0 were investigated in this study at a constant catalyst loading of 0.7 g·L^{-1} (Fig. 7). The decolorization efficiency at pH of 3.0, 6.0, and 10.0 is 90%, 65% and 51%, respectively, after 240 min of reaction. Also the decolorization due to adsorption was measured at pH of 3.0, 6.0, and 10.0. The decolorization efficiencies were 28.2%, 19.6%, and 13.4% in dark, respectively (data not shown). The linear relationships between the ln(C_0/C) and irradiation time were observed under different initial pH values (Fig. 7 (inset)). The rate constants (k_{app}) for the decolorization process decreased from 1.30 × 10^{-2} min^{-1} at pH 3.0 to 0.80 × 10^{-2} min^{-1} at pH 6.0, and to 0.56 × 10^{-2} min^{-1} at pH 10.0, demonstrating that the photocatalytic decolorization of MO was more efficient in the acidic media. MO molecule with sulfuric group normally exists as an anion. The isoelectric point of CdS is close to 5.5 [30], so in the acidic solution, the surface is positively charged, which could enhance the anionic MO sorption through electrostatic interactions and subsequent degradation. The residual amino groups of chitosan in the catalyst might have also contributed to the enhanced MO degradation at a lower pH because the protonation of amino group could similarly introduce more positive charges to the surface, enhancing the sorption of dye anions. The adsorbed MO anions could be oxidized directly by hydroxyl radicals produced in the presence of photocatalyst.

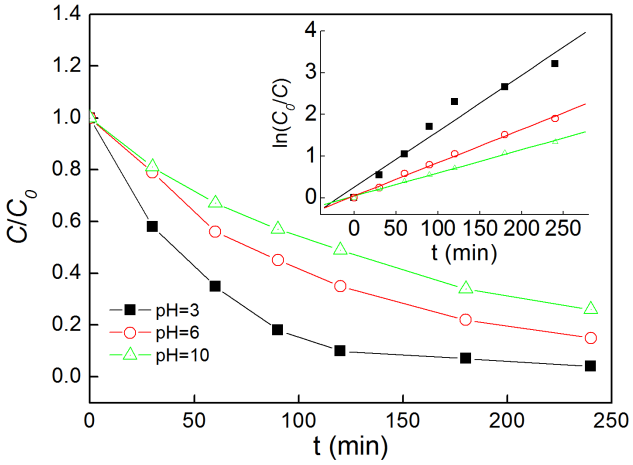

Fig. 7. Effect of pH on the decolorization of MO.

3.7. Reuse of catalyst

To evaluate the lifetime of photocatalyst, the photocatalytic experiments were repeated four times with the same catalyst at an MO concentration of 15 mg·L^{-1} and catalyst loading of 0.7 g·L^{-1}. After 240 min of reaction each time, the catalyst was filtered, washed and recycled. As shown in Fig. 8, the decolorization efficiency for the 4 cycles was 89.7%, 80.3%, 78.6%, and 78.2%, respectively. The catalyst still maintained a high photocatalytic activity after four cycles, suggesting that the chitosan/CdS nanoparticles composite film was relatively stable. Because CdS nanoparticles were synthesized

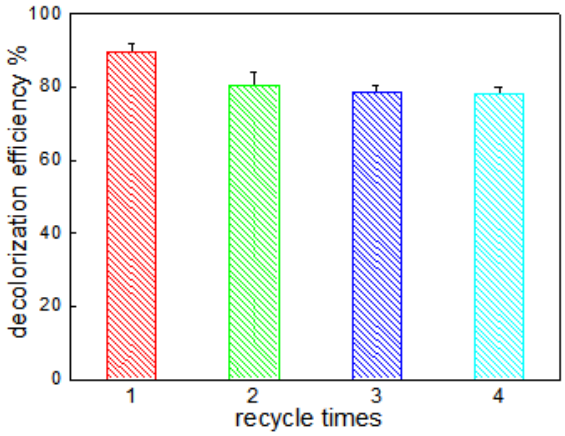

Fig. 8. Stability and recycle of chitosan/CdS nanoparticle composite film.

in chitosan matrices, a large number of active hydroxyl and amino groups in chitosan chains can serve as coordination sites to bind metal ions strongly, which may prevent CdS nanoparticles from agglomeration and photocorrosion during photochemical reaction.

4. Conclusions

In this study, CdS nanoparticles were synthesized *in situ* in the presence of chitosan hydrogel films. The study demonstrated that crosslinked chitosan hydrogel films provided a confined matrix for the growth of CdS nanoparticles and the coordination of Cd^{2+} with $–NH_2$ groups in C_2 and –OH groups in C_3 of the chitosan chain likely occurred. The films can be used effectively for MO photocatalytic decolorization under the UV light irradiation. The photocatalytic process followed apparent pseudo-first-order kinetics. The decolorization of MO solution was more efficiency in the acidic medium. The catalyst could be reused multiple times without significant loss of reactivity.

References

[1] A. Mittal, J. Mittal, A. Malviya, V.K. Gupta, Removal and recovery of Chrysoidine Y from aqueous solutions by waste materials, J. Colloid. Interf. Sci., 344 (2010) 497–507.
[2] V.K. Gupta, R. Jain, S. Varshney, Removal of Reactofix golden yellow 3 RFN from aqueous solution using wheat husk-An agricultural waste, J. Hazard. Mater., 142 (2007) 443–448.
[3] A.K. Jain, V.K Gupta, S. Jain, Suhas, Removal of chlorophenols using industrial wastes, Environ. Sci. Technol., 38 (2004) 4012–4018.
[4] T. Feng, F. Zhang, J. Wang, L. Wang, Application of chitosan-coated quartz sand for congo red adsorption from aqueous solution, J. Appl. Polym. Sci., 125 (2012) 1766–1772.
[5] X. You, F. Chen, J. Zhang, Effects of calcination on the physical and photocatalytic properties of TiO_2 powders prepared by sol–gel template method, J. Sol-Gel. Sci. Technol., 34 (2005) 181–187.
[6] J. Huang, Y. Cao, Z. Deng, H. Tong, Formation of titanate nanostructures under different NaOH concentration and their application in wastewater treatment, J. Solid. State. Chem., 184 (2011) 712–719.
[7] X. Chen, S.S. Mao, Titanium dioxide nanomaterials: synthesis, properties, modifications, and applications, Chem. Rev., 107 (2007) 2891–2959.
[8] C. Pan, Y. Zhu, New type of BiPO4 oxy-acid salt photocatalyst with high photocatalytic activity on degradation of dye, Environ. Sci. Technol., 44 (2010) 5570–5574.
[9] M.R. Hoffmann, S.T. Martin, W. Choi, D.W. Bahnemann, Environmental applications of semiconductor photocatalysis, Chem. Rev., 95 (1995) 69–96.
[10] W.Z. Tang, C.P. Huang, Photocatalyzed oxidation pathways of 2,4-dichlorophenol by CdS in basic and acidic aqueous solutions, Water. Res., 29 (1995) 745–756.
[11] Y. Hu, Y. Liu, H. Qian, Z. Li, J. Chen, Coating colloidal carbon spheres with CdS nanoparticles: microwave-assisted synthesis and enhanced photocatalytic activity, Langmuir, 26 (2010) 18570–18575.
[12] K. Prasad, M. Ashokkumar, Photocatalytic properties of CdS nanoparticles synthesized under various ultrasonic operating conditions, Ind. Eng. Chem. Res., 53 (2014) 715–722.
[13] Y. Hu, X. Gao, L. Yu, J.Q. Wang, S.J. Ning, S. Xu, X.W. Lou, Carbon-coated CdS petalous nanostructures with enhanced photostability and photocatalytic activity, Angew. Chem. Int. Edit., 52 (2013) 5636–5639.
[14] Y. Huo, X. Yang, J. Zhu, H. Li, Highly active and stable CdS–TiO_2 visible photocatalyst prepared by in situ sulfurization under supercritical conditions, Appl. Catal. B: Environ., 106 (2011) 69–75.
[15] F.X. Xiao, J. Miao, B. Liu, Layer-by-Layer Self-Assembly of CdS quantum dots/graphene nanosheets hybrid films for photoelectrochemical and photocatalytic applications, J. Am. Chem. Soc., 136 (2014) 1559–1569.
[16] D. Ke, S. Liu, K. Dai, J. Zhou, L. Zhang, T. Peng, CdS/regenerated cellulose nanocomposite films for highly efficient photocatalytic H_2 production under visible light irradiation, J. Phys. Chem. C., 113 (2009) 16021–16026.
[17] X. Wang, D. Li, Y. Guo, X. Wang, Y. Du, Y. Sun, Preparation of lanthanide doped CdS, ZnS quantum dots in natural polysaccharide template and their optical properties, Opt. Mater., 34 (2012) 646–651.
[18] Z. Li, Y. Du, Z. Zhang, D. Pang, Preparation and characterization of CdS quantum dots chitosan biocomposite, React. Funct. Polym., 55 (2003) 35–43.
[19] R. Jiang, H. Zhu, X. Li, L. Xiao, Visible light photocatalytic decolourization of C. I. Acid Red 66 by chitosan capped CdS composite nanoparticles, Chem. Eng. J., 152 (2009) 537–542.
[20] Y. Li, X. Li, J. Li, J. Yin, Photocatalytic degradation of methyl orange by TiO_2-coated activated carbon and kinetic study, Water. Res., 40 (2006) 1119–1126.
[21] R. Jiang, H. Zhu, G. Zeng, L. Xiao, Y. Guan, Synergy of adsorption and visible light photocatalysis to decolor methyl orange by activated carbor/nanosized CdS/chitosan composite, J. Cent. South. Univ. T., 17 (2010) 1223–1229.
[22] H. Han, R. Bai, Highly effective buoyant photocatalyst prepared with a novel layered-TiO_2 configuration on polypropylene fabric and the degradation performance for methyl orange dye under UV–Vis and Vis lights, Sep. Purif. Technol., 73 (2010) 142–150.
[23] R. Jiang, H. Zhu, J. Yao, Y. Fu, Y. Guan, Chitosan hydrogel films as a template for mild biosynthesis of CdS quantum dots with highly efficient photocatalytic activity, Appl. Surf. Sci., 258 (2012) 3513–3518.
[24] H. Zhu, R. Jiang, L. Xiao, Y. Chang, Y. Guan, X. Li, G. Zeng, Photocatalytic decolorization and degradation of Congo Red on innovative crosslinked chitosan/nano-CdS composite catalyst under visible light irradiation, J. Hazard. Mater., 169 (2009) 933–940.
[25] H. Trabelsi, M. Khadhraoui, O. Hentati, M. Ksibi, Titanium dioxide mediated photodegradation of methyl orange by ultraviolet light, Toxicol. Environ. Chem., 95 (2013) 543–558.
[26] L. Zhang, F. Sun, Y. Zuo, C. Fan, S. Xu, S. Yang, F. Gu, Immobilisation of CdS nanoparticles on chitosan microspheres via a photochemical method with enhanced photocatalytic activity in the decolourisation of methyl orange, Appl. Catal. B: Environ., 156–157 (2014) 293–300.
[27] T. Fan, Y. Li, J. Shen, M. Ye, Novel GQD-PVP-CdS composite with enhanced visible-light-driven photocatalytic properties, Appl. Surf. Sci., 367 (2016) 518–527.
[28] S. Kaur, V. Singh, TiO_2 mediated photocatalytic degradation studies of Reactive Red 198 by UV irradiation, J. Hazard. Mater., 141 (2007) 230–236.
[29] J. Sun, X. Wang, J. Sun, R. Sun, S. Sun, L. Qiao, Photocatalytic degradation and kinetics of Orange G using nano-sized Sn(IV)/TiO_2/AC photocatalyst, J. Mol. Catal. A: Chem., 260 (2006) 241–246.
[30] S. Taşcıoğlu, D. Taş, Surfactant effect on determination of Cu^{2+} and Cd^{2+} ions by ion-selective electrodes providing evidence for the discrepancy between the point of zero charge and the isoelectric point of CdS, Colloids Surf. A: Physicochem. Eng. Asp., 302 (2007) 349–353.